



Warm summers and moderate winter precipitation boost *Rhododendron ferrugineum* L. growth in the Taillefer massif (French Alps)



L. Francon^{a,*}, C. Corona^a, E. Roussel^a, J. Lopez Saez^b, M. Stoffel^{c,d}

^a Université Clermont Auvergne, CNRS, GEOLAB, F-63000 Clermont-Ferrand, France

^b Université Grenoble Alpes, Irstea, UR EMGR, 2 rue de la Papeterie, – BP76, F-38402 St-Martin-d'Hères, France

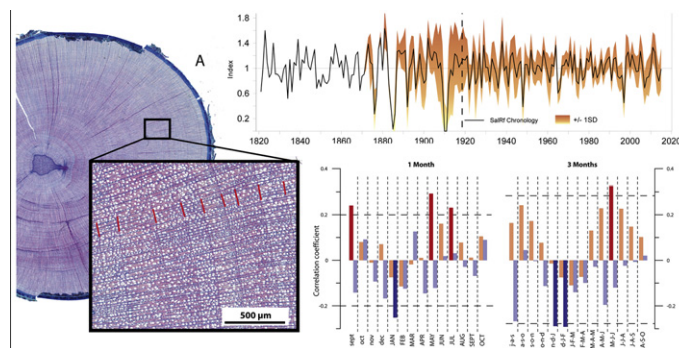
^c Dendrolab.ch, Department of Earth Sciences, University of Geneva, Rue des Maraîchers 13, CH-1205 Geneva, Switzerland

^d Climatic Change and Climate Impacts, Institute for Environmental Sciences, University of Geneva, Boulevard Carl-Vogt 66, CH-1205 Geneva, Switzerland

HIGHLIGHTS

- *Rhododendron ferrugineum* allows the development of multi-decadal annually resolved ring-width chronologies.
- The species allows the reconstruction of climate-growth associations for locations above treeline.
- May–July temperatures are the key unifying growth-limiting factors at the study site.
- *R. ferrugineum* integrates a winter signal in its rings, long-lasting snow cover has a detrimental effect on radial growth.

GRAPHICAL ABSTRACT



ARTICLE INFO

Article history:

Received 24 November 2016

Received in revised form 9 February 2017

Accepted 9 February 2017

Available online 15 February 2017

Editor: Elena Paoletti

Keywords:

Tree-ring analysis

Dwarf shrubs

Rhododendron ferrugineum L.

Climate-growth correlations

Winter precipitation

ABSTRACT

Rhododendron ferrugineum L. is a widespread dwarf shrub species growing in high-elevation, alpine environments of the Western European Alps. For this reason, analysis of its growth rings offers unique opportunities to push current dendrochronological networks into extreme environments and way beyond the treeline. Given that different species of the same genus have been successfully used in tree-ring investigations, notably in the Himalayas where *Rhododendron* spp. has proven to be a reliable climate proxy, this study aims at (i) evaluating the dendroclimatological potential of *R. ferrugineum* and at (ii) determining the major limiting climate factor driving its growth. To this end, 154 cross-sections from 36 *R. ferrugineum* individuals have been sampled above local treelines and at elevations from 1800 to 2100 m asl on northwest-facing slopes of the Taillefer massif (French Alps). We illustrate a 195-year-long standard chronology based on growth-ring records from 24 *R. ferrugineum* individuals, and document that the series is well-replicated for almost one century (1920–2015) with an Expressed Population Signal (EPS) > 0.85. Analyses using partial and moving 3-months correlation functions further highlight that growth of *R. ferrugineum* is governed by temperatures during the growing season (May–July), with increasingly higher air temperatures favoring wider rings, a phenomenon which is well known from dwarf shrubs growing in circum-arctic tundra ecosystems. Similarly, the negative effect of January–February precipitation on radial growth of *R. ferrugineum*, already observed in the Alps on juniper shrubs, is interpreted as a result of shortened growing seasons following snowy winters. We conclude that the strong and unequivocal signals recorded in the fairly long *R. ferrugineum* chronologies can indeed be used for

* Corresponding author.

E-mail address: loic.francon@uca.fr (L. Francon).

climate–growth studies as well as for the reconstruction of climatic fluctuations in Alpine regions beyond the upper limits of present-day forests.

© 2017 Elsevier B.V. All rights reserved.

1. Introduction

Tree-ring series are widely available at high latitudes and high altitudes across the northern hemisphere and represent the backbone of many annually resolved climate reconstructions of the Common Era (Intergovernmental Panel on Climate Change, 2014; Stoffel et al., 2015; Helama et al., 2016; Guillet et al., 2017). At the same time, and as a result of ongoing warming, arctic and alpine environments are also among the most sensitive regions when it comes to their reactions to climate change (e.g. Pauli et al., 2012; Gobiet et al., 2014). So far, however, assessments and time-series of changes in high altitude and high-latitude have been limited mostly to areas where trees (and their growth-ring series) are readily available. Despite the fact that beyond northern and alpine treelines, other woody plants, such as dwarf shrubs, could be useful proxies for paleoclimate and paleoenvironmental reconstructions (Bär et al., 2008), their potential for dendroecological studies has only been explored more fully over the last decade (Myers-Smith et al., 2015b for a detailed review). Although the often extremely narrow rings and numerous anomalies in tree-ring formation making analysis of dwarf shrubs rather difficult and time-consuming (Bär et al., 2008), these pioneering studies also showed that shrub species indeed have a great potential to extend existing dendrochronological networks beyond limits and into extreme environments where trees cannot survive under the current climatic conditions (Liang and Eckstein, 2009). Annual growth rings in shrubs have thus been used among others to reconstruct the growing season climate in Arctic environments (e.g. Schmidt et al., 2006; Weijers et al., 2010) or to explore the rapid climate warming in tundra biomes as a result of the increasing shrub dominance which in turn is related to the evolution of climate–growth relationships (Hallinger et al., 2010; Hollesen et al., 2015; Myers-Smith et al., 2015b).

By contrast to the large body of scientific literature on dwarf shrub studies using circumpolar species, one realizes that dendroecological work on high-elevation shrubs covering multi-decadal timescales remains scarce and that work exploring climate–growth relationships of dwarf shrubs in mountain environments is still largely missing. So far, published work focused mostly on the Tibetan plateau (Liang and Eckstein, 2009; Lu et al., 2015; Liang et al., 2012), the Central Norwegian Scandes (Bär et al., 2008) and the Sierra Nevada (Franklin, 2013). Only one dendroclimatological study has so far been dedicated to the detection of climate signals in shrub-ring chronologies in the Alps on *Juniperus communis* L. (Pellizzari et al., 2014).

To fill this apparent gap and to explore the potential of European high-elevation dwarf shrubs for climate–shrub growth relationships, we directed our attention to *Rhododendron ferrugineum* L. (Ericaceae), an evergreen dwarf shrub with well-branched trailing stems and a height of up to 0.8 m. The species has a large geographic range of occurrence across the Alps (Ozenda, 1985) and is widespread at the subalpine level from about 1600 to 2200 m. In the northwestern Alps, it even forms large heathlands colonizing extensively grazed or abandoned meadows on north, west, and northwest-facing slopes (Escaravage et al., 1997) on which it apparently encounters the most favorable environmental conditions. Its abundance can also be explained by complementary sexual and vegetative reproductive strategies (Doche et al., 2005), which enables *R. ferrugineum* to outcompete other plants (Pornon and Doche, 1996) and to reach a 90–100% cover after 150–250 years (Pornon and Doche, 1995). Based on a simple growth-ring count, Schweingruber and Poschod (2005) documented the existence of a 202-year-old *R. ferrugineum* individual in Central Switzerland, whereas genetic surveys have shown that some genotypes of this long-lived species are estimated to be >300 years old (Escaravage et

al., 1998). Despite its (i) wide distribution, (ii) clearly identifiable annual rings as well as (iii) its longevity, neither its dendroecological potential nor its assumedly reliable climatic signal in its ring-width sequences has been studied so far.

In this context, the objectives of the study are threefold, and consist of (i) assessing the possibility to build a first, and reliable, *R. ferrugineum* ring-width chronology for the Alps; (ii) verifying the sensitivity of the species to climate; and of (iii) comparing *Rhododendron* growth to that of a typical high-elevation tree species in the Alps, namely *Picea abies* (L.) Karst., as this species is typically used in standard dendroecological investigations.

2. Material and methods

2.1. Study site

Samples from *Rhododendron ferrugineum* L. and *Picea abies* (L.) Karst. were sampled at Côte des Salières (45°04'N, 5°88'E, Fig. 1), a site located in the Northern French Alps and within the northwest-facing slopes of the Taillefer massif. According to Ozenda et al. (1968) and Pautou et al. (1992), climate at the study site is reflective of a transition zone between the wettest oceanic pre-alpine environments (Chartreuse, Vercors), where the annual amount of precipitation exceeds 1600 mm at 1000 m asl, and the intra-alpine massif, characterized by a dryer continental climate with annual rainfall <800 mm at Briançon (1400 m asl) (Fig. 1). According to the HISTALP dataset (Chimani et al., 2011), precipitation at the gridded point closest to the study site (45°05'N, 5°85'E) is $1150 \pm 200 \text{ mm} \cdot \text{yr}^{-1}$ for the period 1800–2003. At the same grid point, mean annual temperature is 3.3 °C and mean May–August temperature is 9.9 °C for the period 1780–2008 (Chimani et al., 2013). In the Taillefer massif, snow cover remains in place during 188 days on average, whereas mean snow depth is 66 cm at 1800 m asl for the period 1959–2005 (Durand et al., 2009).

At Côte des Salières, *R. ferrugineum* and *P. abies* samples were collected within the upper subalpine belt, at the treeline ecotone (Holtmeier, 2009) between 1800 and 2100 m asl (Fig. 2). Slope angles range from 23° to 33°. Bedrock primarily consists of amphibolites and gneiss gabbros (Doche et al., 2005), whereas soils are stony ochre brown humic acid soils (Pornon et al., 1997). Monospecific stands of *Picea abies* dominate vegetation to elevations of up to 1850 m asl. The woody understory is mainly composed of *R. ferrugineum* and *Vaccinium myrtillus*. Above 1900 m asl, alpine dwarf shrub heathland has developed on abandoned pastures, dominated by a dense *R. ferrugineum* (80–100%) cover intermixed with individual *Sorbus aucuparia*, *Sorbus chamaemespilus*, and *Vaccinium myrtillus*, along with scattered *Picea abies* and *Pinus uncinata* trees. Significant geomorphic disturbances – related to e.g. snow avalanches or debris flows – are clearly absent.

2.2. Sample collection and preparation

We randomly selected 36 *R. ferrugineum* individuals in fall 2015 above the treeline between 1900 and 2100 m asl. GPS coordinates with ± 1 m accuracy were recorded for each individual using a Trimble GeoExplorer. Two to six cross-sections per individual shrub were saw-cut with lengths each of 20–30 cm. Samples were taken from the main stems departing from the root collar, so that a so-called *serial-sectioning approach*, consisting of ring-width measurements and cross-dating at the intraplant level, can be applied. This approach has been first applied to shrub dendrochronology by Kolishchuk (1990) in an attempt to (i) improve ring-width dating through the identification of wedging

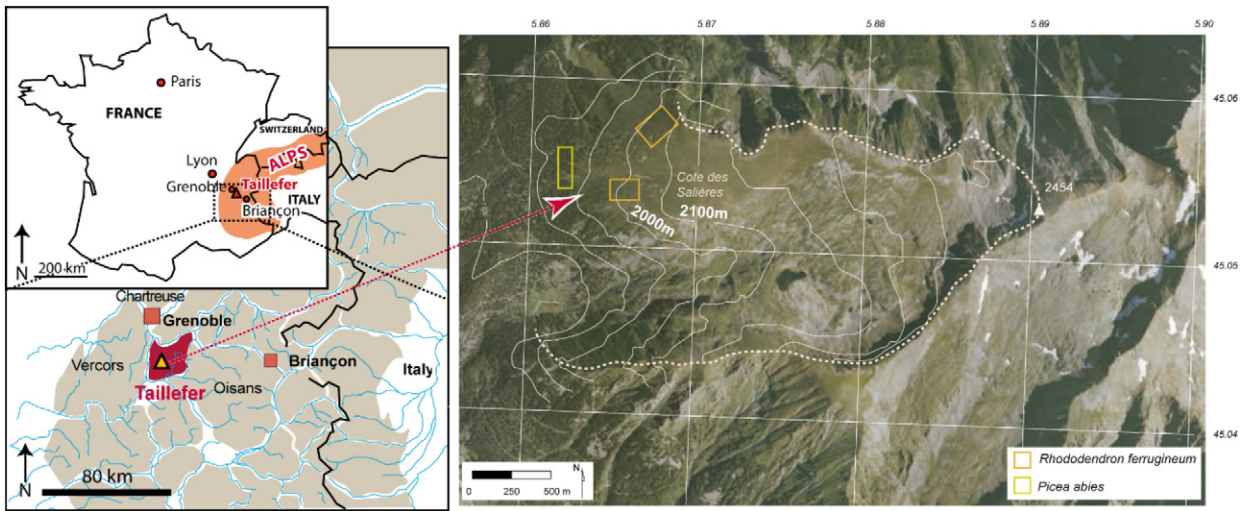


Fig. 1. Location of the study site, called Côte des Salières (SAL, 45°04'N, 5°88'E) in the Massif du Taillefer (French Alps).

and missing rings (Buchwal et al., 2013) as well as continuous missing outer rings which are more likely to occur in large sections of basal stems due to cambial age and growth forms (Wilmking et al., 2012); and to (ii) enhance the common signal and the correlation between individual tree-ring series. In addition, a total of 32 cores from 16 *P. abies* trees (two cores per tree) were taken at the same site using a Suunto increment borer at the lowest possible position on the tree in order to maximize the number of rings. Here, the purpose was to build a conventional tree-ring width chronology which could then be compared to the *R. ferrugineum* chronology.

In total, 106 *R. ferrugineum* micro-sections, with a thickness of ~15–20 μm , were obtained using a slide microtome, stained with a mixture of Safranin and Astra blue and permanently fixed on microslides using Canada balsam (Arbellay et al., 2012; Gärtner et al., 2015). High-resolution digital pictures were captured by a Carl Zeiss Axio Observer Z1 coupled to a Zeiss AxioCam MR R3 camera with 40–100 \times magnification. Individual images were then merged automatically to cover the entire cross-sections. This image merging has been performed with the Zeiss Zen 2011 software (<http://www.zeiss.com/microscopy/int/products/microscope-software/zen-lite.html>).

For *P. abies*, increment cores were mounted on a wooden support, air-dried and sanded with gradually finer sandpapers following standard dendrochronological procedures (Bräker, 2002), thus enhancing

the appearance of ring borders and cell structures. Subsequently, the increment cores were scanned at a resolution of 1200 dpi with a high-resolution Epson 11000XL scanner.

2.3. Cross-dating and chronology development

For both species, tree-ring widths were measured from scanned images with the CooRecorder 7.6 software (Larsson, 2003). In the case of *R. ferrugineum*, ring widths were measured at two to three radii so as to detect wedging or missing rings, but also to enhance the cross-dating between different sections within the same individual. During this procedure, the fact of having as large as possible images of the entire section (rather than images of thin transects) greatly facilitated analysis and helped quite substantially in the detection of partially missing rings.

Radial measurements along chosen radii on individual *R. ferrugineum* samples were supplemented by a careful visual inspection of each cross-section so as to eliminate the risk of growth underestimation caused by partially missing rings. The principal three stages of cross-dating were based on a comparison of growth curves (i) between 2 and 3 radii measured within a single cross-section, (ii) among the mean growth curves of all the sections within the same individual and finally (iii) between the mean growth curves of all individual shrubs was done using C dendro 7.3 (Larsson, 2003). Alignment of growth



Fig. 2. (A) The sampling sites at treeline, more precisely between a *Picea abies* (L.) Karst. (black arrow head) and a *Rhododendron ferrugineum* L. heath. (white arrow head). (B) Illustration of the prostrate growth form of a *Rhododendron* individual growing at high elevation.

curves was based on a visual comparison of positive and negative pointer years as described by Schweingruber (1988). Pointer years refer to cross-dated growth rings presenting common, yet conspicuous ring widths such as exceptionally narrow or wide rings (Schweingruber et al., 1990). The visual cross-dating was then checked statistically in COFECHA (Holmes, 1994).

For *P. abies*, individual series coming from the same tree were cross-checked visually and statistically using Cdendro (Larsson, 2003), so as to check for potential counting errors or missing rings; samples were then corrected if necessary. Individual corrected series were then averaged into a single mean series per tree. In a second step, mean series of different trees were cross-dated with one another and also checked for counting errors or missing rings using Cdendro and COFECHA.

Mean tree ring-width series were then detrended using the dplR package (Bunn, 2008) for R software (R Core Team, 2016) in order to eliminate non-climatic trends (e.g., age related growth trend and/or effect of natural or human-induced disturbances) and to maximize climatic information. The ring-width data from both species were standardized (Fritts, 1976; Cook and Kairiukstis, 1990) following an identical two-step procedure: a double-detrending process was applied based on (i) a negative exponential or linear regression, followed by (ii) a fitting of a cubic smoothing spline with a 50% frequency response at 32 years (Cook and Peters, 1981). Dimensionless indices were obtained by dividing the observed ring-width value by the predicted value. This process allowed the creation of stationary time series for each individual tree with a mean of 1 and a homogeneous variance. Finally, and for each species, growth indices were averaged by year using a bi-weight robust mean which reduces the influence of outliers (Cook and Peters, 1981). They also allowed the development of mean standardized chronologies (SalRf and SalPa for *Rhododendron ferrugineum* L. and *Picea abies* (L.) Karst., respectively) which represent the common high-frequency variation of the individual series (Cook, 1987).

By means of several descriptive statistics – commonly used in dendrochronology – the two species chronologies were compared. These statistics included standard deviation (SD), which estimates the variability of measurements for the whole series; mean sensitivity (MS), which is an indicator of the mean relative change between consecutive ring widths and is calculated as the absolute difference between consecutive indices divided by their mean value, mean RBAR, which is a measure of the common variance between the single series in a chronology and first order autocorrelation (Auto Corr.), a measure of the influence

of previous year's conditions on the following ring formation (Fritts, 1976). The Expressed Population Signal (EPS) was calculated for both the SalRf and SalPa chronologies to indicate the level of coherence of the constructed chronology and to illustrate how it portrays the hypothetical perfect population chronology that has been infinitely replicated from the individual series composing the chronology (Briffa, 1995). The running RBAR and running EPS were computed using a 30-year moving window for both species. Their values illustrate changes in the strength of common patterns of tree growth over time. The commonly accepted EPS threshold of 0.85 (Wigley et al., 1984) is the limit at which tree-ring widths chronologies were considered as reliable and well replicated.

2.4. Climate-growth analysis

The *R. ferrugineum* and *P. abies* chronologies were regressed against mean monthly air temperature (°C) and monthly precipitation totals (mm) using values from the HISTALP dataset. At the grid point 45°05' N, 5°85'E, monthly mean temperature and precipitation totals exhibit statistically significant correlations (wrt. 1920–2003, $p < 0.01$) in May (−0.76), June (−0.73), July (−0.77), August (−0.75), September (−0.76) and October (−0.70).

The exploration of climate–growth relationships between climatic parameters and the *R. ferrugineum* and *P. abies* chronologies was conducted in three methodological steps. First, partial and moving 3-months correlation functions were computed using the seasonal correlation procedure (SEASCORR) developed by Meko et al. (2011) to disentangle confounding influences of correlated climatic variables. SEASCORR in fact correlates tree-ring series with a primary climate variable (i.e., temperature) and uses partial correlations to investigate a secondary variable (i.e., precipitation) controlling for the influence of the primary variable. We selected temperature as the primary variable because previous works examining climate controls on trees at high-altitude sites in the Alps have identified temperature as a key driver (Büntgen et al., 2006; Corona et al., 2011; Saulnier et al., 2011). We then used individual monthly as well as seasonal values integrating three consecutive months (e.g. DJF, MAM, JJA, SON). We considered a 14-month window, thus assessing a period extending from September of the year preceding growth-ring formation ($n - 1$) to October of the year of actual ring formation (n); this approach therefore results in a dataset of 28 climatic variables being analyzed. Confidence intervals

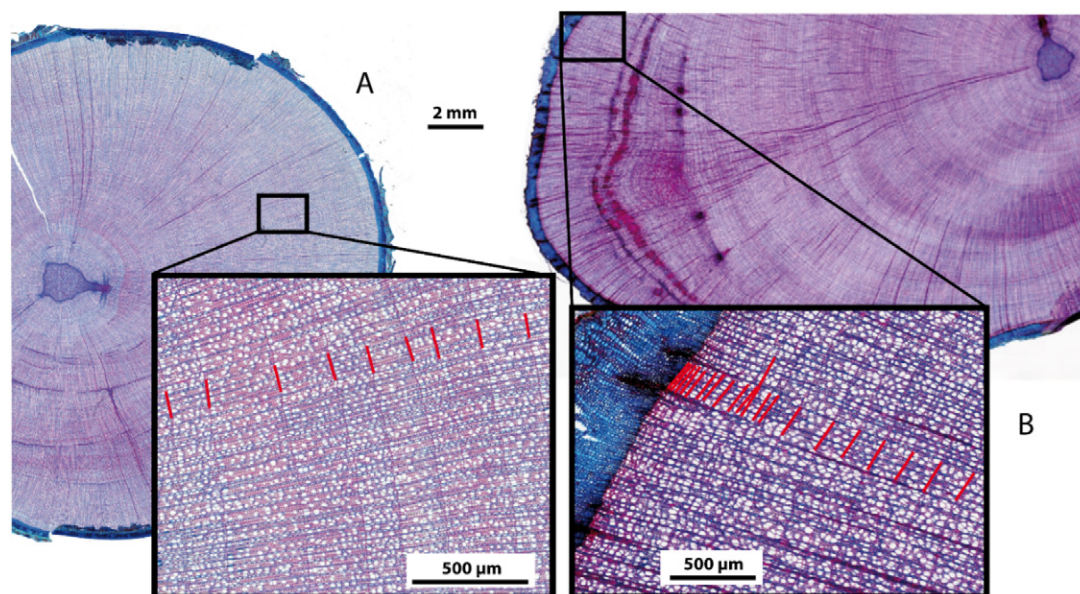


Fig. 3. Examples of cross-sections of *Rhododendron ferrugineum* L. (A) Individuals showing wide, distinct, and concentric rings as well as (B) eccentric, narrow and wedging rings, in the latter case on a cross-section exhibiting 195 growth rings.

for all correlations were estimated by using Monte Carlo simulations of the tree-ring series (Percival and Constantine, 2006). The Bonferroni method was used for multiple comparison correction of the significance levels (Hochberg, 1988).

In a second step, we (i) tested whether the significant growth-climate relationships detected during the SEASCORR analyses are indeed reliable across regional-scale climate variability and (ii) identify potential large-scale forcing effects on tree growth. To this end, we correlated the tree and shrub chronology data with mean monthly temperature and precipitation totals from the HISTALP gridded dataset for all grid cells available in a user-defined region (43–46°N, 4–18°E) and over the time period 1920–2003. Analyses were conducted with the KNMI Climate Explorer (Royal Netherlands Meteorological Institute; <http://www.climexp.knmi.nl>) (van Oldenborgh et al., 2009).

Lastly, we categorized calendar years as pointer years if at least 50% of the cross-dated *R. ferrugineum* and *P. abies* individuals presented an absolute value of radial growth variation exceeding 40% (Mérian and Lebourgeois, 2011). In this study, radial growth variation (RGV) is an expression of the degree to which the ring of the current year (n) is narrower (negative value) or wider (positive value) than the previous

ring (n – 1). The RGV was calculated using the following equation:

$$RGV_n = 100 * \frac{RW_n - RW_{n-1}}{RW_{n-1}} \quad (1)$$

where RW_n is the ring width in year n, and RW_{n-1} indicates ring width of the previous year. The negative pointer years detected in SalRf and SalPa were compared to records of temperature and precipitation from the HISTALP database for the period extending from September (n – 1) to October (n).

3. Results

3.1. Wood anatomical characteristics of *Rhododendron ferrugineum* L.

High-resolution digital pictures from cross-sections display distinctly visible growth rings as annual as a result of the strong climatic seasonality in this alpine ecotone. Growth-ring boundaries are clearly visible and can be discriminated by a band of radially aligned, thick-walled latewood fibers, flattened along the ring boundary. The flattened

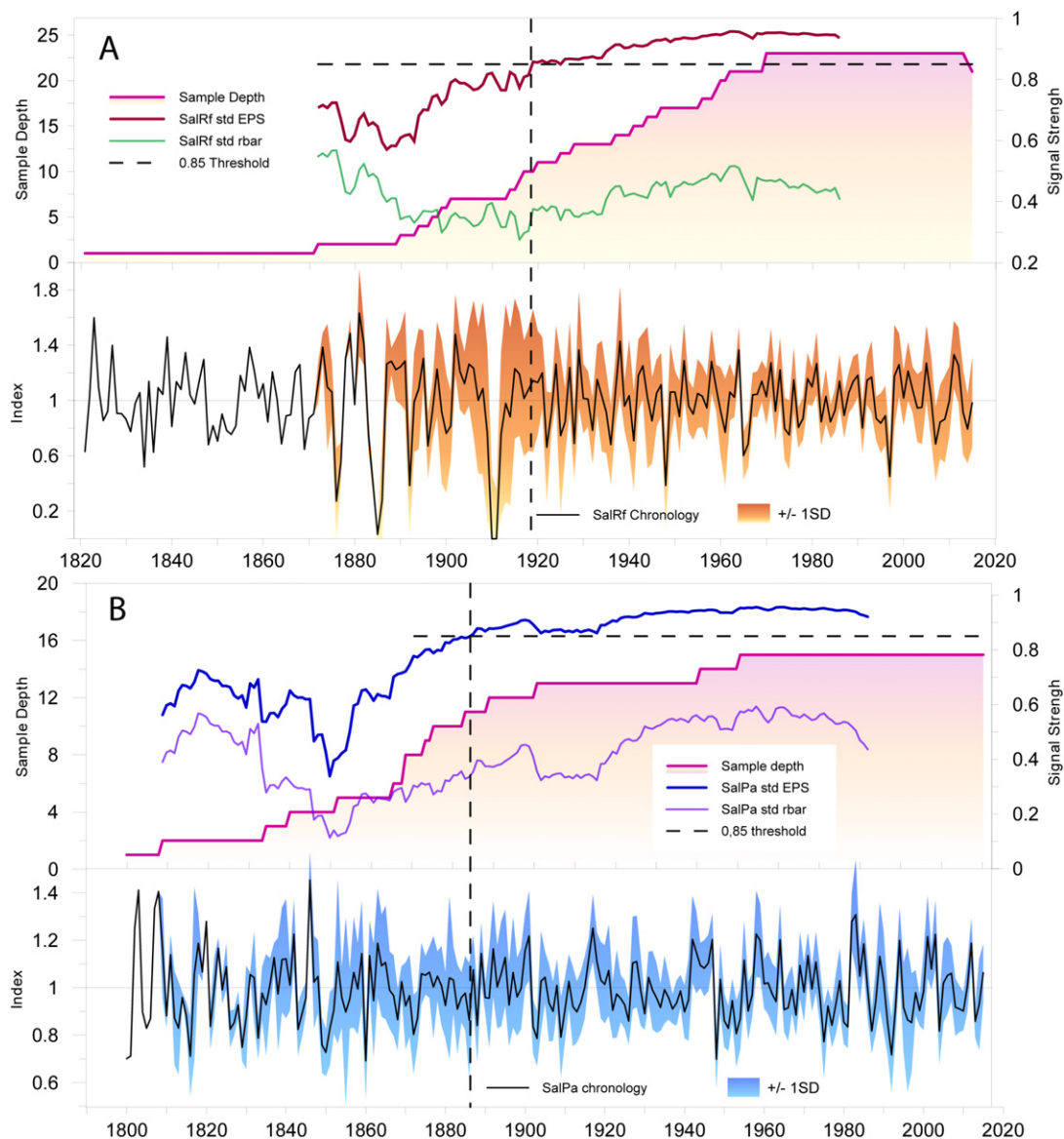


Fig. 4. Standard growth-ring chronology of (A) *Rhododendron ferrugineum* L. and (B) *Picea abies* (L.) Karst at Côte des Salières. Sample depth, running Expressed Population Signal (EPS) and common variance between single tree-ring series in a chronology (RBAR) are computed using a 30-year moving window. Horizontal lines indicate sample depth. The EPS threshold value of 0.85 is passed to the right of the dashed vertical lines (For values exceeding 0.85, a chronology is considered well replicated and reliable).

Table 1

Characteristics of standard *R. ferrugineum* and *P. abies* ring-width chronologies: length, standard deviation, mean sensitivity, first order autocorrelation and signal strength along the entire chronology (i.e. RBAR and EPS).

Species	First year	Last year	Year EPS > 0.85	Mean length	Length	Stand. dev.	Mean sens.	Auto Corr.	RBAR	EPS
<i>R. ferrugineum</i>	1821	2015	1919	81	195	0.27	0.30	0.224	0.41	0.88
<i>P. abies</i>	1800	2015	1887	144	216	0.14	0.14	0.165	0.44	0.89

fibers are in a sharp contrast to the high density of vessels in the remainder of the ring. Ring widths range between 0.1 and 0.3 mm and are rather uniform around the circumference, thus revealing that one-sided, mechanical stress had a rather weak influence on radial growth, at least in the stems selected for this analysis. Despite this concentricity, wedging rings – which often correspond to missing ring in some other parts of the same plant – were rather common. The proportion of completely missing rings was, by contrast, much smaller and only accounted for 2.3% (Fig. 3).

3.2. Cross-dating and chronology statistics

Based on the assessment of 24 individuals (69 sections, rejection rate: 33%), we were able to build a *R. ferrugineum* chronology for the Côte des Salières covering the period 1821–2015 (Fig. 4A). The mean age of individuals included is 91 years, but we counted 195 growth rings on the oldest *R. ferrugineum* individual. By comparison, the *P. abies* chronology was obtained from 16 trees (rejection rate: 0%, mean age of trees: 144 years) and spans 216 years, i.e. the period from 1800 to 2015, with SalRf being characterized by a high common signal represented by an overall RBAR of 0.41 and an average mean sensitivity of 0.3 (Table 1). The expressed population signal (EPS), which is a function of the mean inter-series correlation and series replication, varied from 0.71 to 0.96 (mean = 0.88) and exceeds the threshold of 0.85 ever since 1920 (Fig. 4A).

Fig. 4B denotes the temporal signal strength of SalPa. Except for the period 1800–1887, during which the sample replication is <10 series, EPS (mean: 0.89) and RBAR (mean: 0.44) values point to internal consistency (EPS > 0.85) in common variance between 1887 and 2015. The mean sensitivity (MS) of the SalPa series shows values of 0.17, which are significantly lower than those obtained for SalRf.

The correlation coefficient between SalRf and SalPa is 0.4 ($p < 0.05$) for the 1920–2015 common period characterized by EPS values >0.85.

3.3. Monthly and moving 3-months climate correlations

Partial and moving 3-months correlation functions using monthly mean temperature and monthly totals from September of the year preceding ring formation ($n - 1$) to October of the year of ring formation (n) as climatic variables are presented for *R. ferrugineum* and *P. abies*, respectively (Fig. 5A and B). With respect to monthly values, a significant positive correlation ($p < 0.05$; 1920–2003) is observed between the *R. ferrugineum* ring-width chronology and current May (0.29) and July (0.23) mean temperatures. Significant seasonal (3-months) correlations are also consistently identified for growing season temperatures (MJJ, 0.33). In addition, correlation profiles evidence positive values between SalRf and temperature for September ($n - 1$) (0.24, $p < 0.05$). With respect to monthly and seasonal precipitation totals, significant negative correlation coefficients are found between the standardized *R. ferrugineum* chronology and precipitation totals of January (-0.25 , $p < 0.05$) and more generally of early winter (i.e. NDJ and DJF, -0.29 and -0.29 respectively, $p < 0.05$).

P. abies and *R. ferrugineum* correlation profiles are similar for the current (i.e. April–September) growing season. Significant positive correlations between *P. abies* radial growth and mean air temperature are computed for June (n) and July (n), peaking in July (n) (0.44, $p < 0.05$). In sharp contrast to *R. ferrugineum*, *P. abies* does neither show any sensitivity towards winter and summer precipitation nor

does it react to conditions occurring at the end of the growing period (i.e. in autumn of year n).

3.4. Existence of a regional climatic signal in the SalRf chronology

Correlations coefficients ($p < 0.05$) computed between the SalRf and SalPa chronologies and the gridded HISTALP (43–46°N, 4°–18°E) current May (n)–July (n) mean air temperatures, as well as previous December ($n - 1$)–current February (n) and current May (n)–July (n) precipitation totals are mapped for the period 1920–2003 (Fig. 6). Longer-range correlations obtained with mean air temperatures exceed those derived from precipitation totals. Both chronologies show similar correlation patterns with current May–July mean temperatures throughout a large part of the Greater Alpine Region (Fig. 6A, B). In the case of SalPa, a stronger temperature signal ($0.4 < r < 0.5$) extends from the French Alps to the westernmost parts of the Austrian Alps, this signal ($0.4 < r < 0.3$) is weaker for SalRf.

The precipitation field represented by the SalRf and SalPa data shows generally lower correlations as compared to those derived for mean air temperatures. The spatial correlation patterns with gridded precipitation also differ between species. The SalRf chronology is associated with a winter precipitation field north of approximately 43–49° latitude and with a 4–10°E west-east extension; the core region of the precipitation field is slightly smaller (44–46.5°N, 4–6°E) and centered over the French Alps ($r > 0.3$, $p < 0.05$, Fig. 6C). The SalPa chronology does not, by contrast, show any significant correlation with previous December ($n - 1$)–current February (n) precipitation totals (Fig. 6D).

3.5. Climate during extreme years

For either chronology, years with negative indices – i.e. years where at least 50% of the cross-dated trees presented an absolute value of radial growth variation exceeding 40% – were categorized as extreme and compared to meteorological records of the HISTALP database. The SalRf chronology shows negative pointer years in 1922, 1928, 1948, 1965, and 1997 (Fig. 7). Conversely, the *P. abies* population only shows 1948 as a negative pointer year. Both species exhibit the sharpest and most widespread growth decline in 1948 when 76.5% of the *R. ferrugineum* individuals show a mean RGV of -62.1% and half of the *P. abies* individuals show a RGV of -41% . When compared with monthly data from the HISTALP database, these extremes can be explained by below-average precipitation totals during at least 2–3 winter months. By way of example, precipitation deficits were most significant in 1997 (February–March: -156 mm, February–April: -197 mm), 1948 (February–March: -180 mm), 1965 (January–February: -97 mm) and 1928 (November–December: -161 mm). For the years 1948 and 1997, the effect of precipitation deficits was further enhanced by above-average mean air temperatures between January and May ($+1.6$ and $+1.8$ °C, respectively).

Temperature during the growing season did not apparently have a significant impact on radial growth in the years mentioned above, as no specific climatic parameter could be isolated to explain these pointer years. Whereas negative growing season (May–September) mean air temperature anomalies prevailed in 1948 (-0.7 °C wrt. 1961–1990) and 1965 (-0.75 °C), we note fairly mild conditions during the extreme pointer year of 1928 ($+0.6$ °C) and 1997 ($+0.7$ °C).

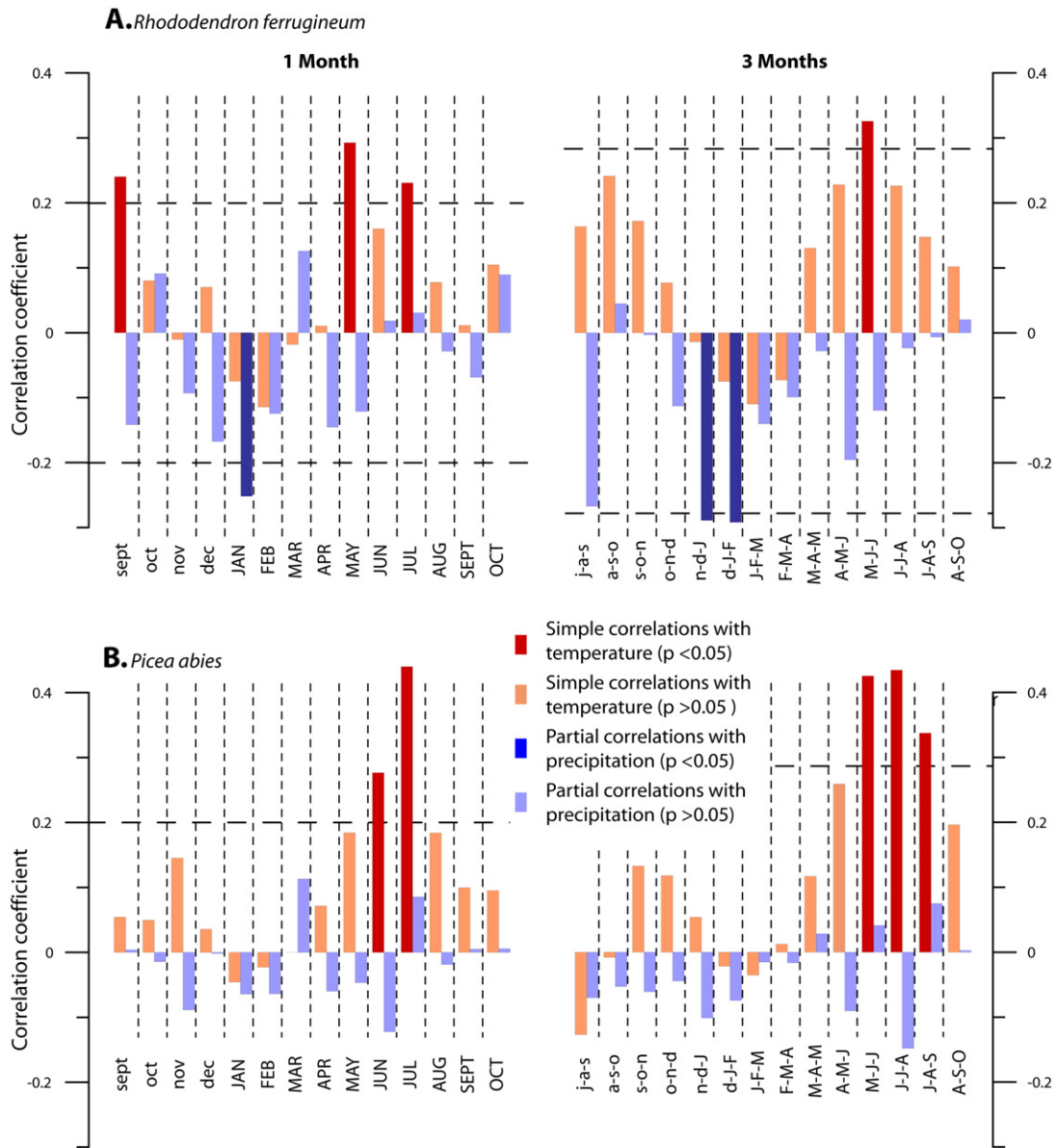


Fig. 5. Monthly and moving 3-months correlation functions (SEACORR) analysis between the *R. ferrugineum* (A, top panel) and *P. abies* (B, bottom panel) chronologies, with monthly mean temperatures and monthly precipitation totals for the period 1920–2003. Simple correlations of tree-ring indices were computed for the primary climate variable (temperature), whereas partial correlations were determined for the secondary climate variable (precipitation).

4. Discussion

4.1. Chronology quality

We present one of the first dendroclimatic investigations from a dwarf shrub in the European Alps and the longest record for a Western European high-altitude species so far. From 24 individuals of *Rhododendron ferrugineum* L., a rather widespread dwarf shrub growing close and above treeline we were able to build a solid reference chronology ($EPS > 0.85$) extending back to the early decades of the 20th century (1920–2015) and responding to summer temperatures and early winter precipitation totals.

At our study site, located around 2000 m asl in the French Alps, *R. ferrugineum* is characterized by rather low growth rates, even lower than those obtained for *R. przewalskii* in the Miyaluo Forest Region ($0.5 \text{ mm} \cdot \text{yr}^{-1}$, Li et al., 2013), *R. aganiphum* ($0.3 \text{ mm} \cdot \text{yr}^{-1}$, Lu et al., 2015) or *R. nivale* on the south-eastern Tibetan Plateau ($0.35 \text{ mm} \cdot \text{yr}^{-1}$, Liang and Eckstein, 2009). In addition, we observe

that wedging or completely missing rings are common in our samples and likely related to the limited length of the growing season as well as to limited resource availability during certain years (Hallinger et al., 2010). Despite these difficulties, a detailed serial sectioning and cross-dating analysis at the shrub level enabled the development of a robust ring-width chronology with relatively high values for the mean inter-series correlation ($RBAR = 0.41$), therefore confirming a common high frequency variance (Fritts, 1976) in the SalRf record. Interestingly, the mean sensitivity of SalRf is significantly larger than that of SalPa and also exceeds values obtained for other *Rhododendron* spp. in the Himalaya (0.21, 0.14–0.19 and 0.12 for *R. przewalskii*, *R. aganiphum* and *R. nivale*, respectively). MS at our study site is comparable to values reported for the only other dwarf shrub chronology published for the Alpine space, *Juniperus communis* (Pellizzari et al., 2014). Nevertheless, it remains generally lower than those of the majority of other shrub chronologies assembled to date in subarctic regions, where e.g. *Salix* spp. (e.g. Schmidt et al., 2006; Blok et al., 2011), *Betula nana* (Blok et al., 2011), or *Juniperus nana* (Hallinger et al., 2010) exhibited mean

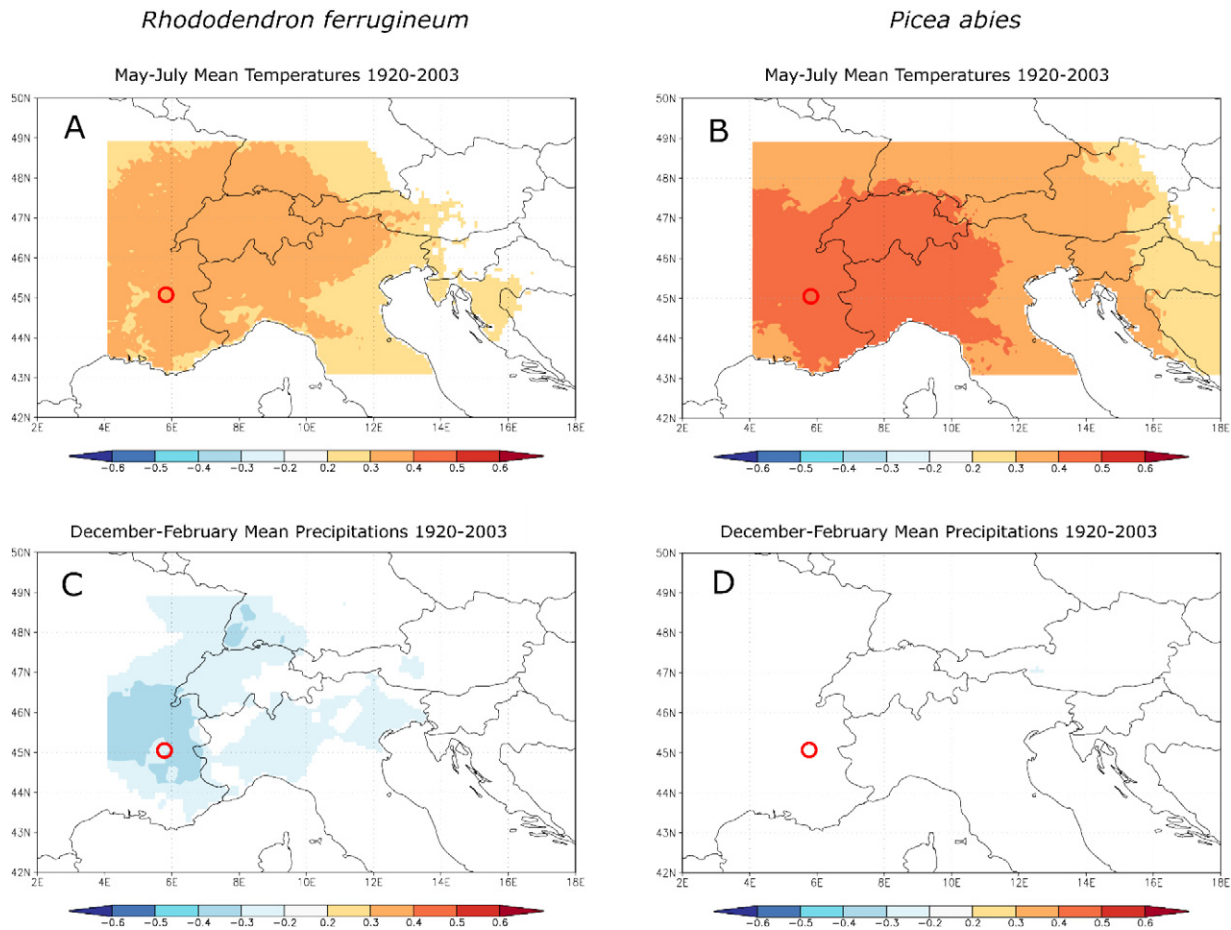


Fig. 6. Spatial correlations ($p < 0.05$) between *R. ferrugineum* (left panel) and *P. abies* (right panel) standard ring-width chronologies and current (n) May–July temperatures (A–B), previous ($n - 1$) December–current (n) February (C–D). Red dots correspond to the location of the study site SAL. Data consist of gridded ($5' \times 5'$ lat/long) surface temperatures and have been extracted from the HISTALP dataset (available at <http://www.zamg.ac.at/histalp>).

sensitivity values $MS > 0.4$, thereby suggesting that tree-ring width in the Taillefer massif did not vary to the same degree from year to year as in the subarctic shrublands.

4.2. Radial growth sensitivity to growing season temperatures and length

We realize that radial growth of *R. ferrugineum* in the Taillefer massif portrays a statistically significant coherence with average temperatures during the growing season on a regional scale. A rather similar dependence on average temperatures during the growing season is observed for SalPa, but also for other networks of conifer tree chronologies sampled at treeline sites across the French Alps (e.g. Corona et al., 2010; Petitcolas, 1998; Rolland et al., 1998; Saulnier et al., 2011). The same coherence with growing season temperatures is also apparent in various *R. ferrugineum* chronologies from the Himalayas (Li et al., 2013; Liang and Eckstein, 2009; Lu et al., 2015) as well as for dwarf shrub chronologies sampled across 37 arctic and alpine sites across the Northern Hemisphere (Myers-Smith et al., 2015a). Table 2 synthesizes the monthly climate-growth correlations (from previous ($n - 1$) September to current (n) October) found in previously published dendroecological studies and classify results according to study regions going from driest to wettest. The data in Table 2 confirm the strong correlations between shrub growth and summer temperatures at the much colder and drier Arctic sites (Myers-Smith et al., 2015a), but also points to much weaker correlations between shrub chronologies and summer temperatures in

typically wetter mountain environments (e.g. Li et al., 2013; Pellizzari et al., 2014).

Partial correlations reveal the predominant role of temperature (May) in driving radial growth of *R. ferrugineum*. This statistical evidence is in good agreement with observations on *Rhododendron aganniphum* cambial activity (Li et al., 2016) and shoot development. In fact, Pornon et al. (1997) demonstrated that shoot development started around mid-June in 1991 and 1992 in the Taillefer massif. Furthermore, higher temperatures in May will favor faster snowmelt. We thus hypothesize that snowmelt indeed modulates the length of the growing season in *R. ferrugineum* and that early snowmelt can effectively boost radial growth. Similar beneficial effects of early snowmelt have been reported for other dwarf shrub species, such as *Juniperus communis*, in the Italian Alps (Pellizzari et al., 2014). Based on data from experimental plots, in which advanced snowmelt was simulated artificially, *Vaccinium myrtillus* reacted with increased growth to mild winter conditions as well (Rixen et al., 2010), therefore adding further evidence to our hypothesis.

The climatic conditions prevailing at the end of the summer and in early fall (temperature in September) are also determinant for radial growth during the next growing season. A similar dependence of radial growth on fall temperatures has been reported for *Rhododendron nivale* growing on the Tibetan Plateau (Liang and Eckstein, 2009). The authors state that negative correlations between growth-ring width – along with cold and dry conditions in preceding November should be attributed to frost damage to leaves and buds which in turn would reduce root

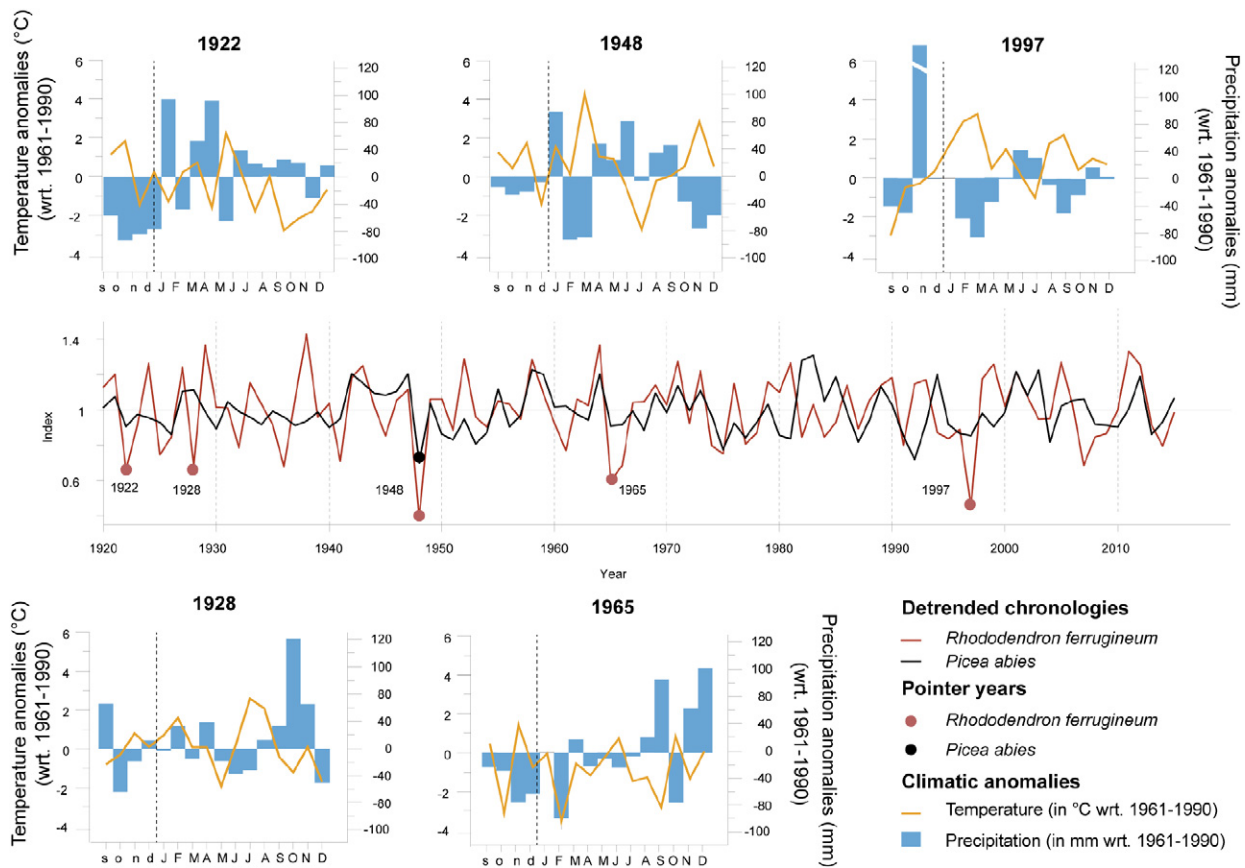


Fig. 7. *Rhododendron ferrugineum* and *Picea abies* detrended chronologies and climatic diagrams of negative extreme years.

activity or increase the risk of frost-induced desiccation. As a consequence, subsequent defoliation and bud mortality would thus deplete the carbon reservoirs and growth hormones and thereby reduce the shrub's potential for further growth and photosynthetic activity.

Apart from *R. nivale*, sensitivity of dwarf shrubs to climatic conditions in early fall have been reported for no other species growing in mountain regions, and thus have to be investigated in future work. Even if comparable studies lack for dwarf shrubs, some literature on the positive effect of previous fall temperatures on radial growth exist in studies focusing on different European conifer species (e.g. Oberhuber, 2004; Carrer et al., 2010; Babst et al., 2012). In the alpine treeline ecotone, Oberhuber (2004) and Oberhuber et al. (2008), for instance demonstrated that *Pinus cembra* trees indeed benefit of warm autumns as unusually mild temperatures will promote mycorrhizal association by maintaining soils above freezing, and will thus also favor maturation of buds against detrimental effects of winter stress. Moreover, some authors assume that high photosynthesis rates late in the fall could lead to high carbon storage and thus to increased growth in the following year (e.g. Fritts, 1976; Babst et al., 2012).

4.3. Contrasted impacts of winter precipitations on radial growth of *R. ferrugineum*

We have also shown that significant negative correlations exist between SalRf and early winter precipitation totals (i.e. previous (n - 1) December–January), both at the local and regional scales. Similar responses have been reported for shrub species and chronologies, such as *Salix arctica* in Greenland (Schmidt et al., 2006, 2010), *Linanthus pungens* in the Sierra Nevada, California (Franklin, 2013), or *Juniperus communis* in the Italian Alps (Pellizzari et al., 2014, 2016) (Table 2). We assume that the extensive and long-lasting snow cover could have a detrimental effect on radial growth of *R. ferrugineum* at our site

through (i) cooler soil temperatures (Pellizzari et al., 2014), (ii) a shortening of the growing season and (iii) possible delays in the onset of cambial activity at the start of the new growing season, or (iv) even through lower amounts of growing degree-days (Vaganov et al., 1999; Blok et al., 2011), which will then be traceable in reduced radial growth of *R. ferrugineum*. In our study, the tree-ring width chronology of *Picea abies* trees does not exhibit this winter signal which tends to validate the hypothesis of physical effects of the snow cover which in fact filter incoming solar radiation (blocking photosynthesis), rather than the collateral reduction in soil temperature (Pellizzari et al., 2014).

As a consequence, the sensitivity of our dwarf shrub species to winter precipitation differs quite sharply from studies in the very dry Arctic ($162 \text{ mm} \cdot \text{yr}^{-1}$) and Himalayan ($210 \text{ mm} \cdot \text{yr}^{-1}$) environments (Zalatan and Gajewski, 2006; Liang et al., 2012) (Table 2) where the positive effects of a thicker snowpack will favor radial growth in shrubs (*Salix alaxensis* and *Juniperus pingii*) as a result of the thermic protective effect against frost (Neuner, 2007) and/or winter desiccation (Sakai and Larcher, 1987). Other studies from these dry sites interpreted the positive effects of a thicker snow cover on radial growth as a result of increased active permafrost layer depth and soil nutrient concentrations during the spring season (Nowinski et al., 2010) which may in turn favor further shrub growth and could thus create positive feedback loops (Sturm et al., 2005; Hallinger et al., 2010; Blok et al., 2011). In the absence of permafrost, however, the mechanisms described above cannot be used to explain enhanced or reduced radial growth in dwarf shrubs in the Alps.

Nevertheless, we observe that several years with very narrow rings in the SalRf chronology coincide with extremely dry winters. Compared to the 1920–2003 mean December–February (DF) precipitation totals, this observation is particularly true for the three last pointer years (1948, 1965 and 1997) for which DF precipitation was significantly lower (131 mm vs 234 mm , $p < 0.05$). In 1922 the occurrence of a

Table 2

Comparisons of shrub chronology responses to climate parameters as published in past studies. The different types of environments are named DA (dry Arctic), HM (high mountain), and O (oceanic). The annual amounts of precipitation are given as well (in mm). Very significant, positive correlations, significant positive correlations and significant negative correlations are respectively indicated with (+++; ++; +; -). Grey boxes point to lacking data.

Authors – Year of publication – studied species		Zalatan and Gajewski, 2006 <i>Salix alaxensis</i>	Buchwal et al. 2013 <i>Salix polaris</i>	Block et al. 2011 <i>Salix pulchra</i>	<i>Betula nana</i>	Hollesen 2015 <i>Betula nana</i>	Hallinger et al. 2010 <i>Juniperus nana</i>	<i>Empetrum hermaphroditum</i>	Forbes et al. 2010 <i>Salix lanata</i>	Au and tardif, 2007 <i>Dryas integrifolia</i>	Jorgensen et al. 2014 <i>Alnus viridis</i>	<i>Salix glauca</i>	Ropars et al. 2015 <i>Betula glandulosa</i>	Liang et al. <i>Juniperus</i> spp	Lu et al. 2015 <i>Rhododendron</i> . Spp.	Li et al. 2013 <i>Rhododendron</i> . Spp.	Liang and Eckstein 2009 <i>R. spp.</i>	Pelizzari et al. 2014 <i>Juniperus communis</i>	Franklin 2013 <i>Linanthus pungens</i>	Beil et al. 2015 <i>Calluna vulgaris</i>	Our study <i>R. ferrugineum</i>		
Type of env.		DA	DA	DA	DA	DA	DA	DA	DA	DA	DA	DA	DA	HM	HM	HM	HM	HM	HM	HM	O	HM	
Mean annual prec.		162	184	203	Same study	273	310	300 to 400	419	432	445	Same study	460	312	672	600 to 1000	836	600 to 1200	1500	1330	1200 to 1800		
MONTH	s	T											+					+				+	
		P																					
	o	T								+													
		P								-													
	n	T																+					
		P		+									-					+		+			
	d	T				+																	
		P	+																				
	J	T															+						
		P												+			+						-
	F	T															+						+
		P																					
	M	T						+															+
		P	+											++									
	A	T																			+		
		P										+		++			-						
	M	T								-				+	-							+	+
		P													+								
	J	T		++	+	+	+	++	++			+	+	+	-						+		+
		P		-											+								
J	T		++	+	+	+	++	++	++		+	+	++		+	+	+			++	++	+	
	P												-										
A	T		++	+			++	++					++								++		
	P																						
S	T																						
	P																						
O	T																						
	P																						

pointer year is coherent with negative precipitation anomalies in November–December months. Only 1928 does not show a dry winter. One should, however, keep in mind that (i) this pointer year is least marked in terms of radial growth variations of the all five pointer years described, (ii) the chronology in 1928 is built with only 13 individuals, and (iii) the precipitation dataset could be inaccurate due to the quality of the measurements back in time and heterogeneity of the precipitation distribution.

For the 1922, 1948, 1965 and 1997 pointer years, we explain this apparent discrepancy with monthly correlations by the increase of winter stress during periods with insufficient snow cover. As winter stress cannot be regarded simply as a number of single stressor-response incidents (Neuner et al., 1999), it is difficult to disentangle, based on pointer analyses alone, the interrelated climatic events inducing an extremely narrow ring. We thus hypothesize that during periods with insufficient snow cover, winter desiccation and freezing damage (Neuner et al., 1999) can occur simultaneously if evergreen *R. ferrugineum* leaves are exposed to excess irradiation, and that limited radial growth can thus occur during the subsequent growing season.

5. Conclusions

We built one of the first dwarf shrub growth-ring chronologies for the European Alps and tested the suitability of the widespread Alpine shrub species *Rhododendron ferrugineum* L. for dendroclimatological investigations. Despite the many challenges encountered during cross-dating, we were able to extract a unique, annually resolved, and statistically solid retrospective of >90 years of *R. ferrugineum* growth variability for a site in the French Alps. The construction of the chronology was facilitated by the well-defined and distinctly visible growth-ring boundaries and by a comprehensive serial sectioning of microcuts from 24 individuals. Results show that a clear climatic signal exists in the growth-ring variability in the growth-ring series. In particular, we observe that the *R. ferrugineum* chronology displays a climate-growth association similar to that observed in treeline *Picea abies* (L.) Karst. trees, with monthly mean May–July temperatures of the current year being the key unifying growth-limiting factors at the study site. In the case of *R. ferrugineum*, warm climatic conditions during previous fall and current May seem to be further influential factors and indeed affect

shrub growth, thus pointing to a clear dependence of ring widths in this dwarf shrub species on the length of the growing season. The early winter (December–February) precipitation signal observed in our *R. ferrugineum* chronology appears to be more complex, as both an extensive and long-lasting snow cover and extremely dry winters seem to have detrimental effects on radial growth.

Given the wide geographic distribution of *R. ferrugineum* and its occurrence above treeline in the Alps, this dwarf shrub species should clearly become a promising candidate and a valuable proxy for the development of multi-centennial, annually resolved ring-width chronologies, even more so as these areas void of trees are typically also lacking meteorological records. In this perspective, we are calling for more research on climate–growth relationships of *R. ferrugineum* and are confident that climate reconstruction from growth-ring records of alpine shrubs can indeed become a standard, high-elevation proxy, even more so if the current study and other initiatives will be enlarged through (i) the development of extensive and dense *R. ferrugineum* chronology networks (Lu et al., 2015), (ii) the use of new anatomical indicators (e.g. earlywood vessel chronologies showing a stronger high-frequency response to climate; von Arx et al., 2016), or (iii) the combination of newly-developed shrub chronologies with other highly resolved proxy data (e.g. lake sediments, glacier mass balance).

Acknowledgements

This research was supported by the program ProXYCliM (2016–2017) funded by the CNRS (Mission interdisciplinarité – RNMSH). *Rhododendron* shrubs and spruce trees were sampled by Christophe Corona, Loïc Francon, Erwan Roussel, Séverine Finet and Robin Mainieri. We are grateful to the UMR PIAF (INRA) for the material provided. We want to thank particularly Thierry Ameglio and Brigitte Girard (UMR PIAF) for their scientific and technical help as well as Olivier Voldoire and Irène Till-Bottraud (GEOLAB). Lastly, we are grateful for the well-thought comments and constructive suggestions made by the reviewers and the editor which helped to improve this manuscript.

References

- Arbellay, E., Corona, C., Stoffel, M., Fonti, P., Decaulne, A., 2012. Defining an adequate sample of earlywood vessels for retrospective injury detection in diffuse-porous species. *PLoS One* 7, e38824. <http://dx.doi.org/10.1371/journal.pone.0038824>.
- Babst, F., Carrer, M., Poulter, B., Urbinati, C., Neuwirth, B., Frank, D., 2012. 500 years of regional forest growth variability and links to climatic extreme events in Europe. *Environ. Res. Lett.* 7:045705. <http://dx.doi.org/10.1088/1748-9326/7/4/045705>.
- Bär, A., Pape, R., Bräuning, A., Löffler, J., 2008. Growth-ring variations of dwarf shrubs reflect regional climate signals in alpine environments rather than topoclimatic differences. *J. Biogeogr.* 35:625–636. <http://dx.doi.org/10.1111/j.1365-2699.2007.01804.x>.
- Blok, D., Sass-Klaassen, U., Schaepman-Strub, G., Heijmans, M.M.P.D., Sauren, P., Berendse, F., 2011. What are the main climate drivers for shrub growth in Northeastern Siberian tundra? *Biogeosciences* 8:1169–1179. <http://dx.doi.org/10.5194/bg-8-1169-2011>.
- Bräker, O.U., 2002. Measuring and data processing in tree-ring research – a methodological introduction. *Dendrochronologia* 20:203–216. <http://dx.doi.org/10.1078/1125-7865-00017>.
- Briffa, K.R., 1995. Interpreting high-resolution proxy climate data: the example of dendroclimatology. In: Von Storch, H., Navarra, A. (Eds.), *Analysis of Climate Variability: Applications of Statistical Techniques*. Springer Berlin Heidelberg, Berlin, pp. 77–94.
- Buchwal, A., Rachlewicz, G., Fonti, P., Cherubini, P., Gärtner, H., 2013. Temperature modulates intra-plant growth of *Salix polaris* from a high Arctic site (Svalbard). *Polar Biol.* 36:1305–1318. <http://dx.doi.org/10.1007/s00300-013-1349-x>.
- Bunn, A.G., 2008. A dendrochronology program library in R (dplR). *Dendrochronologia* 26:115–124. <http://dx.doi.org/10.1016/j.dendro.2008.01.002>.
- Büntgen, U., Frank, D.C., Nievergelt, D., Esper, J., 2006. Summer temperature variations in the European Alps, AD755–2004. *J. Clim.* 19:5606–5623. <http://dx.doi.org/10.1175/JCLI3917.1>.
- Carrer, M., Nola, P., Motta, R., Urbinati, C., 2010. Contrasting tree-ring growth to climate responses of *Abies alba* toward the southern limit of its distribution area. *Oikos* 119:1515–1525. <http://dx.doi.org/10.1111/j.1600-0706.2010.18293.x>.
- Chimani, B., Böhm, R., Matulla, C., Ganekind, M., 2011. Development of a longterm dataset of solid/liquid precipitation. *Adv. Sci. Res.* 6:39–43. <http://dx.doi.org/10.5194/asr-6-39-2011>.
- Chimani, B., Matulla, C., Böhm, R., Hofstätter, M., 2013. A new high resolution absolute temperature grid for the Greater Alpine Region back to 1780. *Int. J. Climatol.* 33:2129–2141. <http://dx.doi.org/10.1002/joc.3574>.
- Cook, E., 1987. The decomposition of tree-ring series for environmental studies. *Tree-Ring Bull.* 47, 37–59.
- Cook, E.R., Kairiukstis, L.A. (Eds.), 1990. *Methods of Dendrochronology*. Springer Netherlands, Dordrecht, Netherlands.
- Cook, E., Peters, K., 1981. The smoothing spline: a new approach to standardizing forest interior tree-ring width series for dendroclimatic studies. *Tree-Ring Bull.* 41, 45–53.
- R Core Team, 2016. R: A Language and Environment for Statistical Computing. R Foundation for Statistical Computing, Vienna, Austria URL: <http://www.R-project.org/>.
- Corona, C., Guiot, J., Edouard, J.L., Chalié, F., Büntgen, U., Nola, P., Urbinati, C., 2010. Millennium-long summer temperature variations in the European Alps as reconstructed from tree rings. *Clim. Past* 6:379–400. <http://dx.doi.org/10.5194/cp-6-379-2010>.
- Corona, C., Edouard, J.-L., Guibal, F., Guiot, J., Bernard, S., Thomas, A., Denelle, N., 2011. Long-term summer (AD751–2008) temperature fluctuation in the French Alps based on tree-ring data: long-term temperature fluctuation in the French Alps. *Boreas* 40:351–366. <http://dx.doi.org/10.1111/j.1502-3885.2010.00185.x>.
- Doche, B., Franchini, S., Pornon, A., Lemperiere, G., 2005. Changes of humus features along with a successional gradient of *Rhododendron ferrugineum* (L.) populations (subalpine level, northwestern Alps, France). *Arct. Antarct. Alp. Res.* 37:454–464. [http://dx.doi.org/10.1657/1523-0430\(2005\)037\[0454:COHFAW\]2.0.CO;2](http://dx.doi.org/10.1657/1523-0430(2005)037[0454:COHFAW]2.0.CO;2).
- Durand, Y., Giraud, G., Latemser, M., Etchevers, P., Méridol, L., Lesaffre, B., 2009. Reanalysis of 47 years of climate in the French Alps (1958–2005): climatology and trends for snow cover. *J. Appl. Meteorol. Climatol.* 48:2487–2512. <http://dx.doi.org/10.1175/2009JAMC1810.1>.
- Escaravage, N., Pornon, A., Doche, B., Till-Bottraud, I., 1997. Breeding system in an alpine species: *Rhododendron ferrugineum* L. (Ericaceae) in the French northern Alps. *Can. J. Bot.* 75:736–743. <http://dx.doi.org/10.1139/b97-084>.
- Escaravage, N., Questiau, S., Pornon, A., Doche, B., Taberlet, P., 1998. Clonal diversity in a *Rhododendron ferrugineum* L. (Ericaceae) population inferred from AFLP markers. *Mol. Ecol.* 7:975–982. <http://dx.doi.org/10.1046/j.1365-294x.1998.00415.x>.
- Franklin, R.S., 2013. Growth response of the alpine shrub, *Linarthus pungens*, to snowpack and temperature at a rock glacier site in the eastern Sierra Nevada of California, USA. *Quat. Int.* 310:20–33. <http://dx.doi.org/10.1016/j.quaint.2012.07.018>.
- Fritts, H.C., 1976. *Tree Rings and Climate*. Academic Press, New York.
- Gärtner, H., Cherubini, P., Fonti, P., von Arx, G., Schneider, L., Nievergelt, D., Verstege, A., Bast, A., Schweingruber, F.H., Büntgen, U., 2015. A technical perspective in modern tree-ring research - how to overcome dendroecological and wood anatomical challenges. *J. Vis. Exp.* 97:1490–1500. <http://dx.doi.org/10.3791/52337>.
- Gobiet, A., Kotlarski, S., Beniston, M., Heinrich, G., Rajczak, J., Stoffel, M., 2014. 21st century climate change in the European Alps—a review. *Sci. Total Environ.* 493:1138–1151. <http://dx.doi.org/10.1016/j.scitotenv.2013.07.050>.
- Guillet, S., Corona, C., Stoffel, M., Khodri, M., Lavigne, F., Ortega, P., Eckert, N., Sielenou, P.D., Daux, V., Churakova (Sidorova), O.V., Davi, N., Edouard, J.-L., Zhang, Y., Luckman, B.H., Myglan, V.S., Guiot, J., Beniston, M., Masson-Delmotte, V., Oppenheimer, C., 2017. Climate response to the Samalas volcanic eruption in 1257 revealed by proxy records. *Nat. Geosci.* 10:123–128. <http://dx.doi.org/10.1038/ngeo2875>.
- Hallinger, M., Manthey, M., Wilmking, M., 2010. Establishing a missing link: warm summers and winter snow cover promote shrub expansion into alpine tundra in Scandinavia. *New Phytol.* 186:890–899. <http://dx.doi.org/10.1111/j.1469-8137.2010.03223.x>.
- Helama, S., Melvin, T.M., Briffa, K.R., 2016. Regional curve standardization: state of the art. *The Holocene* 27:172–177. <http://dx.doi.org/10.1177/0959683616652709>.
- Hochberg, Y., 1988. A sharper Bonferroni procedure for multiple tests of significance. *Biometrika* 75, 800–802.
- Hollesen, J., Buchwal, A., Rachlewicz, G., Hansen, B.U., Hansen, M.O., Stecher, O., Elberling, B., 2015. Winter warming as an important co-driver for *Betula nana* growth in western Greenland during the past century. *Glob. Chang. Biol.* 21:2410–2423. <http://dx.doi.org/10.1111/gcb.12913>.
- Holmes, R.L., 1994. *Dendrochronology Program Library User's Manual*. 1994. Laboratory of Tree-Ring Research, University of Arizona, Tucson, Arizona.
- Holtmeier, F.-K., 2009. Mountain timberlines: ecology, patchiness, and dynamics. *Advances in Global Change Research*, second ed. Springer, Dordrecht Preface.
- Information from paleoclimate archives. In: Intergovernmental Panel on Climate Change (Ed.), *Climate Change 2013 - The Physical Science Basis*. Cambridge University Press, Cambridge, pp. 383–464.
- Kolishchuk, V., 1990. Dendroclimatological study of prostrate woody plant. In: Cook, E.R., Kairiukstis, L.A. (Eds.), *Methods of Dendrochronology Applications in the Environmental Sciences*. Springer Netherlands, Dordrecht, p. 394 [etc.].
- Larsson, L.A., 2003. *CDendro – Cybis Dendro Dating Program*. Cybis Elektron. Data AB Saltsjöbaden Swed.
- Li, Z., Liu, G., Fu, B., Zhang, Q., Ma, K., Pederson, N., 2013. The growth-ring variations of alpine shrub *Rhododendron przewalskii* reflect regional climate signals in the alpine environment of Miyaluo Town in Western Sichuan Province, China. *Acta Ecol. Sin.* 33:23–31. <http://dx.doi.org/10.1016/j.chnaes.2012.12.004>.
- Li, X., Rossi, S., Liang, E., Julio Camarero, J., 2016. Temperature thresholds for the onset of xylogenesis in alpine shrubs on the Tibetan Plateau. *Trees* 30:2091–2099. <http://dx.doi.org/10.1007/s00468-016-1436-z>.
- Liang, E., Eckstein, D., 2009. Dendrochronological potential of the alpine shrub *Rhododendron nivale* on the south-eastern Tibetan Plateau. *Ann. Bot.* 104:665–670. <http://dx.doi.org/10.1093/aob/mcp158>.
- Liang, E., Lu, X., Ren, P., Li, X., Zhu, L., Eckstein, D., 2012. Annual increments of juniper dwarf shrubs above the tree line on the central Tibetan Plateau: a useful climatic proxy. *Ann. Bot.* 109:721–728. <http://dx.doi.org/10.1093/aob/mcr315>.
- Lu, X., Camarero, J.J., Wang, Y., Liang, E., Eckstein, D., 2015. Up to 400-year-old *Rhododendron* shrubs on the southeastern Tibetan Plateau: prospects for shrub-based dendrochronology. *Boreas* 44:760–768. <http://dx.doi.org/10.1111/bor.12122>.

- Meko, D.M., Touchan, R., Anchukaitis, K.J., 2011. Seacorr: a MATLAB program for identifying the seasonal climate signal in an annual tree-ring time series. *Comput. Geosci.* 37:1234–1241. <http://dx.doi.org/10.1016/j.cageo.2011.01.013>.
- Mérian, P., Lebourgeois, F., 2011. Size-mediated climate–growth relationships in temperate forests: a multi-species analysis. *For. Ecol. Manag.* 261:1382–1391. <http://dx.doi.org/10.1016/j.foreco.2011.01.019>.
- Myers-Smith, I.H., Elmendorf, S.C., Beck, P.S.A., Wilmking, M., Hallinger, M., Blok, D., Tape, K.D., Rayback, S.A., Macias-Fauria, M., Forbes, B.C., Speed, J.D.M., Boulanger-Lapointe, N., Rixen, C., Lévesque, E., Schmidt, N.M., Baittinger, C., Trant, A.J., Hermanutz, L., Collier, L.S., Dawes, M.A., Lantz, T.C., Weijers, S., Jørgensen, R.H., Buchwal, A., Buras, A., Naito, A.T., Ravolainen, V., Schaepman-Strub, G., Wheeler, J.A., Wipf, S., Guay, K.C., Hik, D.S., Vellend, M., 2015a. Climate sensitivity of shrub growth across the tundra biome. *Nat. Clim. Chang.* 5:887–891. <http://dx.doi.org/10.1038/nclimate2697>.
- Myers-Smith, I.H., Hallinger, M., Blok, D., Sass-Klaassen, U., Rayback, S.A., Weijers, S., Trant, J.A., Tape, K.D., Naito, A.T., Wipf, S., Rixen, C., Dawes, M.A., Wheeler, J.A., Buchwal, A., Baittinger, C., Macias-Fauria, M., Forbes, B.C., Lévesque, E., Boulanger-Lapointe, N., Beil, I., Ravolainen, V., Wilmking, M., 2015b. Methods for measuring arctic and alpine shrub growth: a review. *Earth-Sci. Rev.* 140:1–13. <http://dx.doi.org/10.1016/j.earscirev.2014.10.004>.
- Neuner, G., 2007. Frost resistance at the upper timberline. In: Wieser, G., Tausz, M. (Eds.), *Trees at Their Upper Limit*. Springer Netherlands, Dordrecht, pp. 171–180.
- Neuner, G., Ambach, D., Aichner, K., 1999. Impact of snow cover on photoinhibition and winter desiccation in evergreen *Rhododendron ferrugineum* leaves during subalpine winter. *Tree Physiol.* 19:725–732. <http://dx.doi.org/10.1093/treephys/19.11.725>.
- Nowinski, N.S., Taneva, L., Trumbore, S.E., Welker, J.M., 2010. Decomposition of old organic matter as a result of deeper active layers in a snow depth manipulation experiment. *Oecologia* 163:785–792. <http://dx.doi.org/10.1007/s00442-009-1556-x>.
- Oberhuber, W., 2004. Influence of climate on radial growth of *Pinus cembra* within the alpine timberline ecotone. *Tree Physiol.* 24. <http://dx.doi.org/10.1093/treephys/24.3.291>.
- Oberhuber, W., Kofler, W., Pfeifer, K., Seeber, A., Gruber, A., Wieser, G., 2008. Long-term changes in tree-ring–climate relationships at Mt. Patscherkofel (Tyrol, Austria) since the mid-1980s. *Trees* 22:31–40. <http://dx.doi.org/10.1007/s00468-007-0166-7>.
- Ozenda, P., 1985. *La végétation de la chaîne alpine dans l'espace montagnard européen*. Masson, Paris; New York; Barcelone.
- Ozenda, P., Tonnell, A., Vigny, F., 1968. Feuille de Vizille (XXXIII - 35). *Doc. Cart. Veget. Alp.* 6, 71–87.
- Pauli, H., Gottfried, M., Dullinger, S., Abdaladze, O., Akhalkatsi, M., Alonso, J.L.B., Coldea, G., Dick, J., Erschbamer, B., Calzado, R.F., Ghosn, D., Holten, J.I., Kanka, R., Kazakis, G., Kollar, J., Larsson, P., Moiseev, P., Moiseev, D., Molau, U., Mesa, J.M., Nagy, L., Pelino, G., Puscas, M., Rossi, G., Stanisci, A., Syverhuset, A.O., Theurillat, J.-P., Tomaselli, M., Unterluggauer, P., Villar, L., Vittoz, P., Grabherr, G., 2012. Recent plant diversity changes on Europe's mountain summits. *Science* 336:353–355. <http://dx.doi.org/10.1126/science.1219033>.
- Pautou, G., Cadel, G., Girel, J., 1992. *Le bassin de Bourg d'Oisans, carrefour phytogéographique des Alpes*. *Rev. Ecol. Alp.* 1, 23–43.
- Pellizzari, E., Pividori, M., Carrer, M., 2014. Winter precipitation effect in a mid-latitude temperature-limited environment: the case of common juniper at high elevation in the Alps. *Environ. Res. Lett.* 9:104021. <http://dx.doi.org/10.1088/1748-9326/9/10/104021>.
- Pellizzari, E., Camarero, J.J., Gazol, A., Granda, E., Shetti, R., Wilmking, M., Moiseev, P., Pividori, M., Carrer, M., 2016. Diverging shrub and tree growth from the Polar to the Mediterranean biomes across the European continent. *Glob. Chang. Biol.* <http://dx.doi.org/10.1111/gcb.13577>.
- Percival, D.B., Constantine, W.L.B., 2006. Exact simulation of Gaussian time series from nonparametric spectral estimates with application to bootstrapping. *Stat. Comput.* 16:25–35. <http://dx.doi.org/10.1007/s11222-006-5198-0>.
- Petitcolas, V., 1998. Dendroécologie comparée de l'épicéa, du mélèze, du pin cembro et du pin à crochets en limite supérieure de la forêt dans les Alpes françaises: influence de la variabilité macro-écologique. Université Joseph Fourier, Grenoble.
- Pornon, A., Doche, B., 1995. Influence des populations de *Rhododendron ferrugineum* L. sur la végétation subalpine (Alpes du Nord-France). *Feddes Repert.* 106:179–191. <http://dx.doi.org/10.1002/fedr.19951060312>.
- Pornon, A., Doche, B., 1996. Age structure and dynamics of *Rhododendron ferrugineum* L. populations in the northwestern French Alps. *J. Veg. Sci.* 7:265–272. <http://dx.doi.org/10.2307/3236327>.
- Pornon, A., Escaravage, N., Till-Bottraud, I., Doche, B., 1997. Variation of reproductive traits in *Rhododendron ferrugineum* L. (Ericaceae) populations along a successional gradient. *Plant Ecol.* 1–11.
- Rixen, C., Schwoerer, C., Wipf, S., 2010. Winter climate change at different temporal scales in *Vaccinium myrtillus*, an Arctic and alpine dwarf shrub. *Polar Res.* 29:85–94. <http://dx.doi.org/10.1111/j.1751-8369.2010.00155.x>.
- Rolland, C., Petitcolas, V., Michalet, R., 1998. Changes in radial tree growth for *Picea abies*, *Larix decidua*, *Pinus cembra* and *Pinus uncinata* near the alpine timberline since 1750. *Trees* 13:40–53. <http://dx.doi.org/10.1007/PL00009736>.
- Sakai, A., Larcher, W., 1987. *Frost Survival of Plants: Responses and Adaptation to Freezing Stress*. Ecological Studies. Springer, Berlin.
- Saulnier, M., Edouard, J.-L., Corona, C., Guibal, F., 2011. Climate/growth relationships in a *Pinus cembra* high-elevation network in the Southern French Alps. *Ann. For. Sci.* 68: 189–200. <http://dx.doi.org/10.1007/s13595-011-0020-3>.
- Schmidt, N.M., Baittinger, C., Forchhammer, M.C., 2006. Reconstructing century-long snow regimes using estimates of high Arctic *Salix arctica* radial growth. *Arct. Antarct. Alp. Res.* 38:257–262. [http://dx.doi.org/10.1657/1523-0430\(2006\)38\[257:RCSRUE\]2.0.CO;2](http://dx.doi.org/10.1657/1523-0430(2006)38[257:RCSRUE]2.0.CO;2).
- Schmidt, N.M., Baittinger, C., Kollmann, J., Forchhammer, M.C., 2010. Consistent dendrochronological response of the dioecious *Salix arctica* to variation in local snow precipitation across gender and vegetation types. *Arct. Antarct. Alp. Res.* 42:471–475. <http://dx.doi.org/10.1657/1938-4246-42.4.471>.
- Schweingruber, F.H., 1988. *Tree Rings*. Springer Netherlands, Dordrecht.
- Schweingruber, F.H., Poschold, P., 2005. Growth rings in herbs and shrubs: life span, age determination and stem anatomy. *For. Snow Landsc. Res.* 79, 195–415.
- Schweingruber, F.H., Eckstein, D., Serre-Bachet, F., Bräker, O.U., 1990. Identification, presentation and interpretation of event years and pointer years in dendrochronology. *Dendrochronologia* 8, 9–38.
- Stoffel, M., Khodri, M., Corona, C., Guillet, S., Poulin, V., Bekki, S., Guiot, J., Luckman, B.H., Oppenheimer, C., Lebas, N., Beniston, M., Masson-Delmotte, V., 2015. Estimates of volcanic-induced cooling in the Northern Hemisphere over the past 1,500 years. *Nat. Geosci.* 8:784–788. <http://dx.doi.org/10.1038/ngeo2526>.
- Sturm, M., Schimel, J., Michaelson, G., Welker, J.M., Oberbauer, S.F., Liston, G.E., Fahnestock, J., Romanovsky, V.E., 2005. Winter biological processes could help convert Arctic tundra to shrubland. *Bioscience* 55:17. [http://dx.doi.org/10.1641/0006-3568\(2005\)055\[0017:WBPHC\]2.0.CO;2](http://dx.doi.org/10.1641/0006-3568(2005)055[0017:WBPHC]2.0.CO;2).
- Vaganov, E.A., Hughes, M.K., Kiryanov, A.V., Schweingruber, F.H., Silkin, P.P., 1999. Influence of snowfall and melt timing on tree growth in subarctic Eurasia. *Nature* 400: 149–151. <http://dx.doi.org/10.1038/22087>.
- van Oldenborgh, G.J., Drijfhout, S., van Ulden, A., Haarsma, R., Sterl, A., Severijns, C., Hazeleger, W., Dijkstra, H., 2009. Western Europe is warming much faster than expected. *Clim. Past* 5:1–12. <http://dx.doi.org/10.5194/cp-5-1-2009>.
- von Arx, G., Crivellaro, A., Prendin, A.L., Čufar, K., Carrer, M., 2016. Quantitative wood anatomy—practical guidelines. *Front. Plant Sci.* 7. <http://dx.doi.org/10.3389/fpls.2016.00781>.
- Weijers, S., Broekman, R., Rozema, J., 2010. Dendrochronology in the high Arctic: July air temperatures reconstructed from annual shoot length growth of the circumpolar dwarf shrub *Cassiope tetragona*. *Quat. Sci. Rev.* 29:3831–3842. <http://dx.doi.org/10.1016/j.quascirev.2010.09.003>.
- Wigley, T.M.L., Briffa, K.R., Jones, P.D., 1984. On the average value of correlated time series, with applications in dendroclimatology and hydrometeorology. *J. Clim. Appl. Meteorol.* 23:201–213. [http://dx.doi.org/10.1175/1520-0450\(1984\)023<0201:OTAVOC>2.0.CO;2](http://dx.doi.org/10.1175/1520-0450(1984)023<0201:OTAVOC>2.0.CO;2).
- Wilmking, M., Hallinger, M., Van Bogaert, R., Kyncl, T., Babst, F., Hahne, W., Juday, G.P., de Luis, M., Novak, K., Völlm, C., 2012. Continuously missing outer rings in woody plants at their distributional margins. *Dendrochronologia* 30:213–222. <http://dx.doi.org/10.1016/j.dendro.2011.10.001>.
- Zalatan, R., Gajewski, K., 2006. Dendrochronological potential of *Salix alaxensis* from the Kuujua river area, Western Canadian Arctic. *Tree-Ring Res.* 62:75–82. <http://dx.doi.org/10.3959/1536-1098-62.2.75>.